Journal of Materials Chemistry A

PAPER

View Article Online
View Journal | View Issue

Cite this: J. Mater. Chem. A, 2014, 2, 2657

A non-fullerene acceptor with all "A" units realizing high open-circuit voltage solution-processed organic photovoltaics†

Lingcheng Chen,[a] Linquan Huang,[ac] Dong Yang,[ac] Shuying Ma,[b] Xin Zhou,[a] Jian Zhang,*[a] Guoli Tu*[b] and Can Li*[a]

Received 29th October 2013
Accepted 1st December 2013

DOI: 10.1039/c3ta14396a

www.rsc.org/MaterialsA

A novel non-fullerene small molecule electron acceptor **TTzBT-DCAO**, which contains all electron-withdrawing units of 2,1,3-benzothiadiazole, oligothiazole and alkyl cyanoacetate, has been synthesized and characterized. Its photophysical, electrochemical, and photovoltaic properties have been investigated. The material has favorable HOMO and LUMO levels of −5.88 and −3.60 eV, and shows strong absorption in the visible spectrum up to 650 nm. The small molecule : non-fullerene bulk-heterojunction organic photovoltaics (OPVs) were constructed based on two small molecules SF8TBT and **TTzBT-DCAO**. The influence of the donor : acceptor composition on device performance was investigated. The open-circuit voltages of the devices are over 1.20 V, which is among the highest values reported for single-junction OPVs. The results indicate that small molecules with all electron-withdrawing units could provide a novel route to efficient solution-processed OPVs with high open-circuit voltages.

Introduction

Solution-processed bulk-heterojunction organic photovoltaics (BHJ OPVs) have been intensively investigated for their advantages of low cost, light weight, and large-area fabrication on flexible substrates.[1–8] Besides the polymer donor materials in OPVs, solution-processed small molecules, linear, discotic, star, and dendritic structures, have attracted much attention very recently, due to their advantages of monodispersity, simple synthesis, efficient purification with standard organic chemistry techniques, and reproducible photovoltaic performance.[9–13] With the rapid development of small molecule OPVs, their power conversion efficiencies (PCEs) are close to that of their polymer counterparts.[14–16] Furthermore, the small molecule BHJ OPVs are often obtained with high open-circuit voltage (V_{oc}) (>0.8 V), which is a crucial parameter to high PCEs.[17–24]

To date, almost all highly efficient solution-processed small molecule OPVs are based on small molecule : fullerene systems because of the large electron affinity, high electron mobility and ultra-fast three-dimensional charge transfer of the fullerenes.[25–29] However, fullerenes have a few obvious disadvantages, such as weak absorption in the visible region, high-cost production and purification.[30–33] Recently, solution-processed small molecule : non-fullerene OPVs, by combining a small molecule donor with a non-fullerene acceptor as an active layer, have gradually attracted attention.[34–38] K. Petritsch *et al.* first reported the solution-processed dye-based donor–acceptor non-fullerene OPVs. They fabricated phthalocyanine–perylene blend cells with a V_{oc} of 0.11 V and a fill factor (FF) of 0.25.[34] Later, they have developed the discotic liquid crystal hexa-perihexabenzocoronene combined with a perylene dye to engineer self-organized photovoltaic structures with the power efficiency maximum of 1.95% under 490 nm illumination at 0.47 mW cm^{-2}.[35] A. Sharenko *et al.* have recently reported a solution-processed small molecule : perylene diimide (PDI) BHJ OPV achieving a PCE of 3.0% in the optimized device.[36] Except for the PDI non-fullerene acceptors, there are rare reports of such systems.[38] In light of these, it is necessary to develop new solution-processed small molecules as non-fullerene acceptor materials and to research structure–property–performance relationships for the fabrication and optimization of small molecule : non-fullerene BHJ OPV systems.

Here we report a novel non-fullerene acceptor material, with 2,1,3-benzothiadiazole as a center core, oligothiazoles as arm groups and alkyl cyanoacetate groups as the end-capped units (**TTzBT-DCAO**, Scheme 1), and the small molecule : non-fullerene BHJ OPVs. Using the simple solution spin-coating fabrication process, SF8TBT was used as the electron donor,[39]

[a]State Key Laboratory of Catalysis, Dalian Institute of Chemical Physics, Chinese Academy of Sciences, Dalian National Laboratory for Clean Energy, 457 Zhongshan Road, Dalian 116023, PR China. E-mail: jianzhang@dicp.ac.cn; canli@dicp.ac.cn
[b]Wuhan National Laboratory for Optoelectronics, Huazhong University of Science and Technology, Wuhan 430074, PR China. E-mail: tgl@mail.hust.edu.cn
[c]Graduate University of Chinese Academy of Sciences, Beijing 100049, PR China

† Electronic supplementary information (ESI) available. See DOI: 10.1039/c3ta14396a

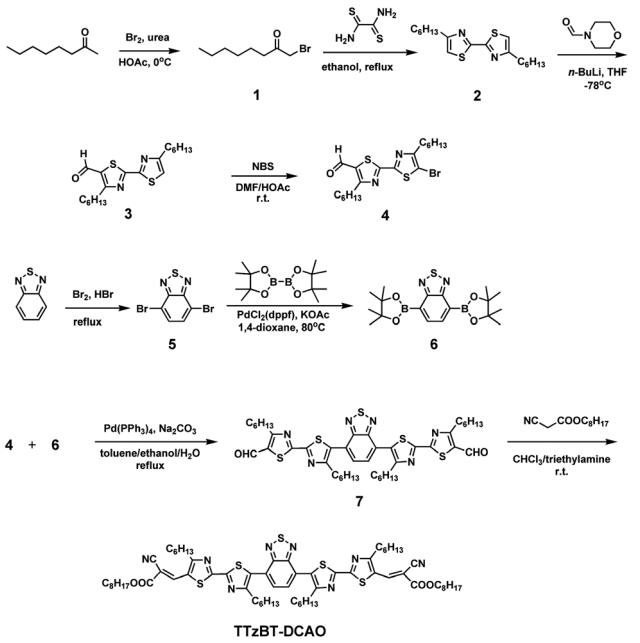

Scheme 1 Synthetic routes for the molecule TTzBT-DCAO.

the device gives a V_{oc} as high as 1.24 V, which is among the highest values reported for single-junction OPVs.

Experimental section

Materials and characterization

All reagents were purchased from Aldrich or Acros and used without further purification. Solvents for chemical synthesis were purified according to the standard procedures. All chemical reactions were carried out under an inert atmosphere. The indium-tin oxide (ITO) on glass was purchased from AimCore Technology Co., Ltd. Poly(3,4-ethylenedioxythiophene) : poly(styrenesulfonate) (PEDOT : PSS) (Clevios 4083) was obtained from H. C. Starck Baytron. ^{1}H NMR and ^{13}C NMR spectra were recorded with a Bruker Avance 400 NMR spectrometer. The mass spectra were recorded using a Bruker Ultraflex III MALDI-TOF/TOF MS instrument. The UV–Vis absorption spectra were measured using a Cary 5000 UV–Vis spectrometer. Solution spectra were recorded in dichloromethane for UV–Vis absorption with a concentration of 10^{-5} M. Thin films on quartz for spectroscopic measurements were prepared by spin-coating. Cyclic voltammetry experiments were performed on a CHI440B potentiostat/galvanostat system. The measurements were carried out with a conventional three-electrode system consisting of a platinum working electrode, a platinum counter electrode, and a Ag/AgCl reference electrode. The supporting electrolyte was 0.1 M tetrabutylammonium hexafluorophosphate (Bu_4NPF_6). Ferrocene was used as a standard to calibrate the system. X-ray diffraction (XRD) patterns were obtained with a D/MAX-2500/PC diffractometer using CuKα radiation at 40 kV and 20 mA. Atomic force microscopy (AFM) images were obtained using a Bruker Metrology Nanoscope III-D atomic force microscope in tapping mode under atmospheric conditions.

Theoretical calculations

Geometry optimizations were carried out by the density functional theory (DFT) at the B3LYP/6-31 G(d) level. All the calculations were performed using the Gaussian 09 program. To simplify the calculation, alkyl chains were replaced by CH_3 groups.

Device fabrication and testing

The ITO glass plates were cleaned in a sonication bath in acetone, isopropyl alcohol and deionized water sequentially, dried by blowing nitrogen, and then treated with O_2 plasma for 15 min before use. A 50 nm thick ITO-modifying layer of PEDOT : PSS was spin-coated on top of ITO and then baked for 15 min at 150 °C. Thin films of active layer were spin-coated from their solution in chlorobenzene. After that, the substrate was transferred to a vacuum thermal evaporator, followed by deposition of the Ca/Al (10 nm/100 nm) cathode at a base pressure of 4×10^{-4} Pa through a shadow mask with an array of 6.2 mm^2 openings. All devices were characterized with a computer-controlled Keithley 2400 source measure unit under AM 1.5 G simulated solar illumination (100 mW cm^{-2}). Incident photon to current efficiency (IPCE) was characterized on the QTest Station 2000ADI system (Crowntech. Inc., USA). The light intensity at each wavelength was calibrated with a standard single-crystal Si photovoltaic cell. All the measurements were performed at room temperature under ambient conditions.

Synthesis

1-Bromo-2-octanone (1). 2-Octanone (40 mL, 0.251 mol), urea (25.0 g, 0.417 mol), and glacial acetic acid (125 mL) were added to a 250 mL two-necked flask with an ice bath for cooling. A solution of bromine (14.0 mL, 0.275 mol) in glacial acetic acid (40 mL) was added dropwise to the flask, and the solution was stirred overnight at room temperature. H_2O (250 mL) was then added to the solution, and the solution was extracted with CH_2Cl_2 (DCM) three times. The organic layer was washed with 10% sodium carbonate, brine, dried over anhydrous $MgSO_4$ and then filtered. The pure product was obtained after vacuum distillation (22.2 g, 42.7%). ^{1}H NMR ($CDCl_3$, 400 MHz, ppm): δ 3.86 (s, 2H), 2.62 (t, J = 7.4 Hz, 2H), 1.62–1.55 (m, 2H), 1.27 (br, 6H), 0.87–0.84 (m, 3H).

4,4′-Dihexyl-2,2′-bithiazole (2). Compound **1** (22.2 g, 108 mmol), dithiooxamide (6.5 g, 55 mmol), and absolute ethanol (280 mL) were added to a 500 mL two-necked flask equipped with a reflux condenser. The solution was heated to reflux for 4 h, and after cooling, it was poured onto crushed ice. The mixture was extracted with DCM three times, washed with H_2O and then dried over anhydrous $MgSO_4$. After the evaporation of the solvent, the pure product was obtained as a brown crystal (14.7 g, 80.8%). ^{1}H NMR ($CDCl_3$, 400 MHz, ppm): δ 6.96 (s, 2H), 2.42 (t, J = 7.6 Hz, 4H), 1.78–1.70 (m, 4H), 1.41–1.30 (m, 12H), 0.91–0.87 (m, 6H).

4,4′-Dihexyl-2,2′-bithiazole-5-carbaldehyde (3). A solution of *n*-BuLi (1.6 M) (6.5 mL, 10.35 mmol) in hexane was added to a solution of compound **2** (3.03 g, 9 mmol) in THF (200 mL) at

−78 °C. After stirring for 1 h, a solution of *N*-formylmorpholine (1.03 mL, 10.35 mmol) in THF (50 mL) was added. After additional stirring for 1 h at −78 °C, the mixture was allowed to warm to room temperature overnight. The final solution was acidified with HCl solution (10 mL) and stirred for 45 min at room temperature. The aqueous phase was extracted with DCM three times, and dried over anhydrous $MgSO_4$. After evaporation of the solvent, the final crude product was purified by column chromatography with petroleum ether (PE)–DCM (1 : 1) to obtain the pure product **3** (2.4 g, 73.2%).

5′-Bromo-4,4′-dihexyl-2,2′-bithiazole-5-carbaldehyde (4). Compound **3** (1.82 g, 5 mmol) was dissolved in a mixture of *N*,*N*-dimethylformamide (30 mL) and glacial acetic acid (30 mL) under nitrogen in the dark, and then NBS (0.99 g, 5.5 mmol) was added dropwise. After 2 h of stirring in the dark, a crude solid precipitated in the reaction mixture. The precipitate was filtered, washed with CH_3OH, and then purified by column chromatography with PE–DCM (3 : 1) to obtain the pure product **4** (1.9 g, 85.6%). ^{1}H NMR ($CDCl_3$, 400 MHz, ppm): δ 10.12 (s, 1H), 3.08 (t, J = 7.6 Hz, 2H), 2.79 (t, J = 7.6 Hz, 2H), 1.84–1.69 (m, 4H), 1.40–1.34 (m, 12H), 0.90 (br, 6H).

4,7-Dibromo-2,1,3-benzothiadiazole (5). 2,1,3-Benzothiadiazole (5.0 g, 36.8 mmol) was added to a 250 mL two-necked flask with hydrobromic acid 75 mL (48%), and the mixture was heated to reflux. A solution of bromine (17.6 g, 110 mmol) in hydrobromic acid 50 mL was added dropwise very slowly. After completion of the bromine addition, the reaction mixture was refluxed for 6 h and a great deal of needle crystals precipitated. Then the mixture was cooled down to room temperature, filtered, and washed with H_2O several times, and then the solid was recrystallized using chloroform. The pure product **5** was obtained as pale yellow crystals (8.0 g, 74%). ^{1}H NMR ($CDCl_3$, 400 MHz, ppm): δ 7.69 (s, 2H).

2,1,3-Benzothiadiazole-4,7-bis(boronic acid pinacol ester) (6). A solution of compound **5** (1 g, 3.41 mmol), bis(pinacolato) diboron (2 g, 7.8 mmol), $PdCl_2$(dppf) (500 mg, 0.6 mmol), and KOAc (2 g, 20 mmol) in degassed 1,4-dioxane (15 mL) was stirred at 80 °C overnight. The reaction was quenched by adding H_2O and the resulting mixture was washed with ethyl acetate three times. The organic layers were washed with brine, and dried over anhydrous $MgSO_4$. After evaporation of the solvent, the final crude product was purified by column chromatography with 3% ethyl acetate in hexane to obtain the pure product **6** (0.53 g, 40.1%). ^{1}H NMR ($CDCl_3$, 400 MHz, ppm): δ 8.12 (s, 2H), 1.43 (s, 24H).

2,1,3-Benzothiadiazole-4,7-bis(4,4′-dihexyl-2,2′-bithiazole-5-carbaldehyde) (7). Compound **4** (1.10 g, 2.5 mmol), compound **6** (0.4 g, 1.0 mmol), $Pd(PPh_3)_4$ (145 mg), Na_2CO_3 (2 M) were dissolved in toluene (60 mL)/EtOH (6 mL)/H_2O (6 mL) and the mixture was refluxed for 24 h. After evaporating the solvent under reduced pressure, H_2O (50 mL) and DCM (50 mL) were added. The aqueous phase was extracted with DCM three times, and the organic layer was dried over anhydrous $MgSO_4$. After evaporation of the solvent, the final crude product was purified by column chromatography with DCM to obtain the pure product **7** (0.60 g, 69.8%). ^{1}H NMR ($CDCl_3$, 400 MHz, ppm): δ 10.15 (s, 2H), 7.82 (s, 2H), 3.12 (t, J = 7.6 Hz, 4H), 2.91 (t, J = 7.2 Hz, 4H), 1.85 (s, 8H), 1.42–1.27 (m, 24H), 0.90 (s, 6H), 0.84 (s, 6H).

TTzBT-DCAO. Compound **7** (0.17 g, 0.2 mmol) was dissolved in a solution of dry $CHCl_3$ (20 mL) and two drops of triethylamine and then octyl cyanoacetate (0.40 g, 2.0 mmol) were added and the resulting solution was stirred for 24 h, under argon, at room temperature. The reaction mixture was then extracted with DCM three times, washed with H_2O and dried over anhydrous $MgSO_4$. After evaporation of the solvent, the final crude product was purified by column chromatography with PE–DCM (1 : 1) to obtain the pure product **TTzBT-DCAO** as a black solid (0.22 g, 89.9%). ^{1}H NMR ($CDCl_3$, 400 MHz, ppm): δ 8.45 (s, 2H), 7.83 (s, 2H), 4.33 (t, J = 6.6 Hz, 4H), 3.00 (t, J = 7.5 Hz, 4H), 2.94 (t, J = 7.5 Hz, 4H), 1.91–1.76 (m, 12H), 1.44–1.29 (m, 44H), 0.91–0.85 (m, 18H). ^{13}C NMR ($CDCl_3$, 400 MHz, ppm): δ 169.82, 166.34, 163.31, 160.02, 159.08, 154.25, 144.09, 131.39, 130.14, 127.70, 125.98, 116.02, 101.57, 67.53, 32.42, 32.18, 31.37, 30.96, 30.71, 30.13, 29.83, 29.60, 29.20, 26.46, 23.29, 23.23, 23.18, 14.73, 14.69. MS (MALDI-TOF): calcd for $C_{66}H_{90}N_8O_4S_5$ $[M]^+$, 1219.80; found, 1220.07.

Results and discussion

Synthesis and characterization

The synthetic routes for the molecules are outlined in Scheme 1. Compound **TTzBT-DCAO** was synthesized from the Suzuki coupling reaction and the Knoevenagel condensation reaction with octyl cyanoacetate in a high yield. Their structures were verified by ^{1}H NMR, ^{13}C NMR spectroscopy and mass spectrometry. The small molecule was soluble in common organic solvents including dichloromethane, chloroform, toluene and chlorobenzene. Also, XRD experiments reveal that the molecule **TTzBT-DCAO** has a crystalline structure with a sharp diffraction peak at $2\theta = 5.5°$ (Fig. S1†).

Photophysical properties

Fig. 1 shows the normalized spectra of optical absorption of **TTzBT-DCAO** in dichloromethane solution (10^{-6} M) and solid films. The absorption spectrum of the solution shows two absorption peaks at 308 and 456 nm, respectively, covering a broad wavelength range from 300 to 650 nm, which is benefited from its π-functional molecular structure. The weak peak absorption is corresponding to the n→π* transition and the peak wavelength of the main absorption peak corresponds to

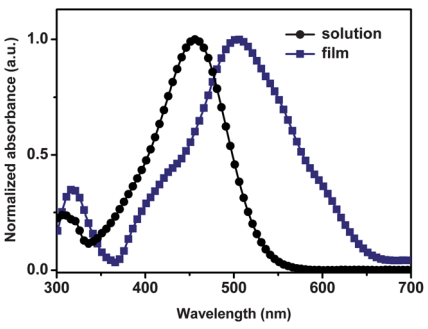

Fig. 1 UV–Vis absorption spectra in DCM solution and as spin-coated films.

the intramolecular charge-transfer (ICT) transition. The absorption onset of 560 nm corresponds to an estimated optical gap of 2.21 eV. A thin film of **TTzBT-DCAO** shows a significant broad absorption of 300–650 nm with two peaks at 318 and 504 nm, and the maximum peak red shifts 48 nm relative to that in solution because of the strong intermolecular interactions.

Electrochemical properties

In order to investigate the electrochemical energy levels of the molecule, cyclic voltammetry (CV) measurements were performed (Fig. S2†). A more complete study of the reversible reductions is shown in Fig. 2a. The highest occupied molecular orbital (HOMO) level and the lowest unoccupied molecular orbital (LUMO) level are estimated from the onset oxidation potential and the onset reduction potential relative to the reference energy level of Fc/Fc^+ (4.80 eV below vacuum). **TTzBT-DCAO** exhibits one irreversible oxidation and two reversible reduction waves. Estimated from the onsets of oxidation, the molecule shows a deep HOMO energy of −5.88 eV, which could prevent the hole transporting to the cathode, while it shows two reversible reduction potentials of −1.20 and −1.50 V, which can be ascribed to the reduction of benzothiadiazole and thiazole units. From the onset reduction value, the LUMO energy is estimated to be −3.60 eV. The favorable LUMO level, higher than that of (6,6)-phenyl-C60-butyric acid methyl ester ($PC_{61}BM$) of −3.91 eV, is desirable for obtaining higher V_{oc} in the OPVs.[40] Thus, the electrochemical bandgap is 2.28 eV, which is close to the optical bandgap.

To obtain further insights into the electronic structure of the compound **TTzBT-DCAO**, its geometry was optimized by density functional theory calculations at the B3LYP/6-31 G(d) level. As shown in Fig. 2b, the electron density distribution of the HOMO is mainly located on the whole conjugated molecule. When the oxidation reaction occurs on the molecule, double bonds in the main chain could be broken due to losing electrons. The electron density of the LUMO is also distributed over the whole molecule with higher density on the electron-deficient benzothiadiazole and thiazole units. When the reduction reaction occurs on the molecule, the more accessible positions of the free electron are benzothiadiazole and thiazole units. Also, the molecule is not only the reactant of the oxidation reaction, but also the product of the reduction reaction in the electrochemical experiments. Therefore, the calculated HOMO and LUMO levels of −5.81 eV and −3.35 eV could be used for estimating the reaction redox potentials. Furthermore, the alternating distribution of the electron density from the HOMO and LUMO orbitals is a benefit for the electron transporting. These theoretical results are consistent with the experimental data.

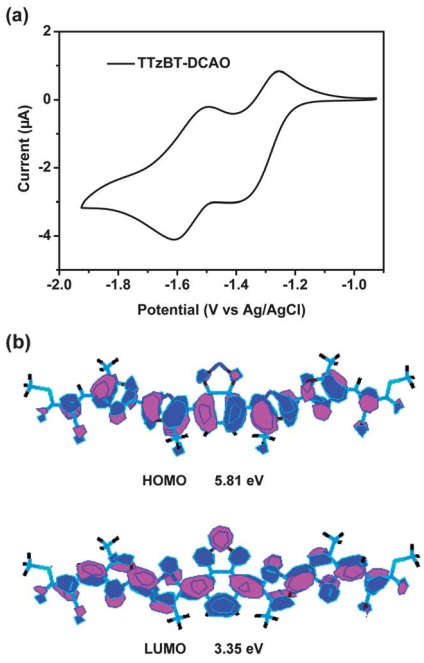

Fig. 2 Cyclic voltammograms in DCM solution of 0.1 M Bu_4NPF_6 with a scan rate of 100 mV s^{-1} (a), and theoretically calculated HOMO and LUMO levels (b).

Photovoltaic properties

The small molecule : non-fullerene BHJ OPVs of the conventional structure of ITO/PEDOT : PSS/SF8TBT : **TTzBT-DCAO**/Ca/Al were fabricated without any thermal annealing and high boiling temperature additive in the solutions, in which **TTzBT-DCAO** was used as the electron acceptor while SF8TBT was used as the electron donor (Fig. 3). The influence of blend composition was investigated using five different weight ratios of 1 : 0.5, 1 : 0.75, 1 : 1, 1 : 1.25 and 1 : 1.5 while the optimized film thickness of the active layer is about 100 nm. The V_{oc}, short circuit current density (J_{sc}), FF, and PCE under AM 1.5 G simulated solar illumination (100 mW cm^{-2}) are listed in Table 1.

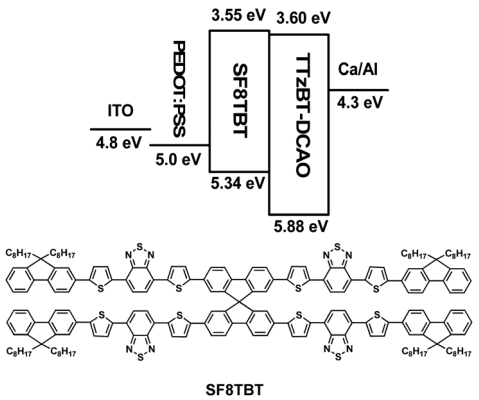

Fig. 3 Schematic diagram of OPVs and the molecular structure used in the devices.

Table 1 Photovoltaic performances of the OPVs

Blend ratio(D/A)	V_{oc} [V]	J_{sc} [mA cm^{-2}]	FF	PCE [%]
1 : 0.5	1.21	0.24	0.32	0.09
1 : 0.75	1.23	0.25	0.33	0.11
1 : 1	1.24	0.47	0.35	0.21
1 : 1.25	1.24	0.17	0.28	0.06
1 : 1.5	1.21	0.05	0.05	0.003

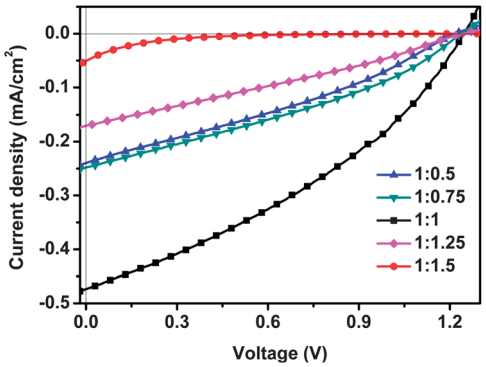

Fig. 4 Current density–voltage (J–V) curves of the OPVs based on SF8TBT : **TTzBT-DCAO**.

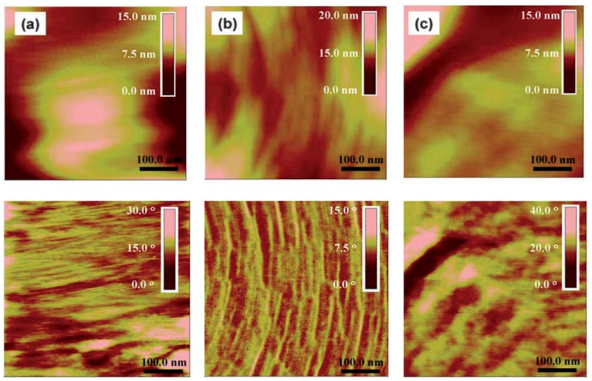

Fig. 5 AFM height (500 × 500 nm, top) and phase images (500 × 500 nm, bottom) of the active layers based on SF8TBT : **TTzBT-DCAO** with different blend ratios: 1 : 0.5 (a), 1 : 1 (b), and 1 : 1.5 (c).

Fig. 4a shows the current density–voltage (J–V) curves of the device characteristics based on the different donor–acceptor weight ratios. As we expected, these devices afforded relatively high V_{oc} values (>1.20 V), which is mainly attributed to the very large difference (1.74 eV) between the LUMO level of **TTzBT-DCAO** and the HOMO level of SF8TBT.[41] Encouragingly, the blend at the donor–acceptor weight ratio of 1 : 1 exhibited a very high V_{oc} of up to 1.24 V, which is among the highest values reported for single-junction BHJ OPVs. Simultaneously, the J_{sc}, FF and PCE reach 0.47 mA cm^{-2}, 0.35 and 0.21%, respectively. The incident photon to current efficiency (IPCE) curve of the best performance device was measured as well (Fig. S3†). The device exhibited significant photo-to-current responses in the range of 350–650 nm based on the weight ratio of 1 : 1. The IPCE spectra correspond to the absorption spectra of **TTzBT-DCAO** and SF8TBT.[39] The integrated short circuit current from the IPCE spectra is 0.44 mA cm^{-2} that is consistent with the experimental data.

To demonstrate the electron mobility of the molecule **TTzBT-DCAO**, the electron-only device structure of ITO/titanium diisopropoxide bis(2,4-pentanedionate) (TIPD) (10 nm)/**TTzBT-DCAO** (150 nm)/Ca/Al was designed (Fig. S4†). In the trap-free region over the trap-filled limit, which is the limit of the presence of carrier traps, space charge limited current (SCLC) can be characterized by the Mott–Gurney square law,[42]

$$J = (9/8)\varepsilon_r\varepsilon_0\mu_e(V^2/L^3)$$

where ε_0 is the vacuum permittivity, ε_r is the dielectric permittivity of the active layer, L is the thickness of the active layer, and μ_e is the electron mobility. At a typical electric field of 10^5 V cm^{-1} (corresponding to an applied voltage of 1 V across a 100 nm thick device), the apparent electron mobility calculated from the currents in the square law region of 2.34×10^{-5} cm^2 V^{-1} s^{-1} has been determined for the device.

The low J_{sc}, leading to the low efficiency, may be due to the small difference (0.05 eV) between the LUMO level of **TTzBT-DCAO** and the LUMO level of SF8TBT.[38] Normally, a difference larger than 0.3 eV is needed for an efficient exciton dissociation.[43] From the J–V curves based on the device of the weight ratio 1 : 1, we calculated the series resistance of 950 Ω cm^2, which may be another reason for the low J_{sc}. In combination with small molecule donor materials having a higher LUMO level, the J_{sc} could be improved and therefore the PCEs. Further studies on this system are under way and will be presented in a forthcoming paper.

The active layer morphologies were examined by AFM in tapping mode. As shown in Fig. 5, the AFM images of the three blend films exhibit different smooth surfaces with the aggregated domains. An interpenetrating network can be observed on the surface of the blend films with the blend ratio of 1 : 1, which should be beneficial to charge separation and transportation in the OPV devices. It proves that the higher J_{sc} is beneficial to the more orderly arrangement.

Conclusions

In summary, a novel non-fullerene electron acceptor material, which contains all electron-withdrawing units, has been synthesized and characterized. The material exhibits a high LUMO level of −3.60 eV and broad absorption-attractive properties compared to the widely used fullerene acceptors. By blending with a small molecule donor material, we demonstrate small molecule : non-fullerene BHJ OPVs with a very high V_{oc} of 1.24 V, which is among the highest values reported for single-junction OPVs. Although the efficiency is not high, these initial results demonstrate that small molecules with all electron-withdrawing units could provide a novel route to high performance solution-processed OPVs with high open-circuit voltages.

Acknowledgements

This work was financially supported by the National Natural Science Foundation of China under grant no. 20904057 and 21374120, and Solar Energy Initiative of the Knowledge Innovation Program of the Chinese Academy of Sciences under grant no. KGCX2-YW-395-2. J. Zhang acknowledges support by 100 Talents Program of the Chinese Academy of Sciences.

Notes and references

1 J. G. Yu, J. Gao, J. C. Hummelen, F. Wudl and A. J. Heeger, *Science*, 1995, **270**, 1789–1791.
2 B. C. Thompson and J. M. J. Frechet, *Angew. Chem., Int. Ed.*, 2008, **47**, 58–77.
3 D. Gendron and M. Leclerc, *Energy Environ. Sci.*, 2011, **4**, 1225–1237.
4 C.-L. Ho and W.-Y. Wong, *Coord. Chem. Rev.*, 2011, **255**, 2469–2502.
5 T. Ameri, P. Khoram, J. Min and C. J. Brabec, *Adv. Mater.*, 2013, **25**, 4245–4266.
6 Z. He, C. Zhong, S. Su, M. Xu, H. Wu and Y. Cao, *Nat. Photonics*, 2012, **6**, 593–597.
7 J. You, L. Dou, K. Yoshimura, T. Kato, K. Ohya, T. Moriarty, K. Emery, C.-C. Chao, J. Gao, G. Li and Y. Yang, *Nat. Commun.*, 2013, **4**, 1446.
8 W. Li, A. Furlan, K. H. Hendriks, M. M. Wienk and R. A. J. Janssen, *J. Am. Chem. Soc.*, 2013, **135**, 5529–5532.
9 B. Walker, C. Kim and T.-Q. Nguyen, *Chem. Mater.*, 2011, **23**, 470–482.
10 A. Mishra and P. Bäuerle, *Angew. Chem., Int. Ed.*, 2012, **51**, 2020–2067.
11 Y. Lin, Y. Li and X. Zhan, *Chem. Soc. Rev.*, 2012, **41**, 4245–4272.
12 J. Zhou, X. Wan, Y. Liu, Y. Zuo, Z. Li, G. He, G. Long, W. Ni, C. Li, X. Su and Y. Chen, *J. Am. Chem. Soc.*, 2012, **134**, 16345–16351.
13 Y. Sun, G. C. Welch, W. L. Leong, C. J. Takacs, G. C. Bazan and A. J. Heeger, *Nat. Mater.*, 2012, **11**, 44–48.
14 G. Wei, S. Wang, K. Sun, M. E. Thompson and S. R. Forrest, *Adv. Energy Mater.*, 2011, **1**, 184–187.
15 J. Zhou, Y. Zuo, X. Wan, G. Long, Q. Zhang, W. Ni, Y. Liu, Z. Li, G. He, C. Li, B. Kan, M. Li and Y. Chen, *J. Am. Chem. Soc.*, 2013, **135**, 8484–8487.
16 V. Gupta, A. K. K. Kyaw, D. H. Wang, S. Chand, G. C. Bazan and A. J. Heeger, *Sci. Rep.*, 2013, **3**, 1965.
17 H. Shang, H. Fan, Y. Liu, W. Hu, Y. Li and X. Zhan, *Adv. Mater.*, 2011, **23**, 1554–1557.
18 P. Dutta, W. Yang, S. H. Eom, W. H. Lee, I. N. Kang and S. H. Lee, *Chem. Commun.*, 2012, **48**, 573–575.
19 P. Li, H. Tong, J. Ding, Z. Xie and L. Wang, *J. Mater. Chem. A*, 2013, **1**, 8805–8812.
20 H. Shang, H. Fan, Y. Liu, W. Hu, Y. Li and X. Zhan, *J. Mater. Chem.*, 2011, **21**, 9667–9673.
21 Y. Liu, X. Wan, F. Wang, J. Zhou, G. Long, J. Tian and Y. Chen, *Adv. Mater.*, 2011, **23**, 5387–5391.
22 T. S. van der Poll, J. A. Love, T. Q. Nguyen and G. C. Bazan, *Adv. Mater.*, 2012, **24**, 3646–3649.
23 B. Walker, A. B. Tomayo, X. D. Dang, P. Zalar, J. H. Seo, A. Garcia, M. Tantiwiwat and T. Q. Nguyen, *Adv. Funct. Mater.*, 2009, **19**, 3063–3069.
24 H. Bürckstümmer, E. V. Tulyakova, M. Deppisch, M. R. Lenze, N. M. Kronenberg, M. Gsänger, M. Stolte, K. Meerholz and F. Würthner, *Angew. Chem., Int. Ed.*, 2011, **50**, 11628–11632.
25 F. G. Brunetti, X. Gong, M. Tong, A. J. Heeger and F. Wudl, *Angew. Chem., Int. Ed.*, 2010, **49**, 532–536.
26 F. G. Brunetti, R. Kumar and F. Wudl, *J. Mater. Chem.*, 2010, **20**, 2934–2948.
27 R. B. Ross, C. M. Cardona, D. M. Guldi, S. G. Sankaranarayanan, M. O. Reese, N. Kopidakis, J. Peet, B. Walker, G. C. Bazan, E. Van Keuren, B. C. Holloway and M. Drees, *Nat. Mater.*, 2009, **8**, 208–212.
28 G. Zhao, Y. He and Y. Li, *Adv. Mater.*, 2010, **22**, 4355–4358.
29 Y. He and Y. Li, *Phys. Chem. Chem. Phys.*, 2011, **13**, 1970–1983.
30 A. L. Roes, E. A. Alsema, K. Blok and M. K. Patel, *Prog. Photovolt.: Res. Appl.*, 2009, **17**, 372–393.
31 J. Kalowekamo and E. Baker, *Sol. Energy*, 2009, **83**, 1224–1231.
32 T. D. Nielsen, C. Cruickshank, S. Foged, J. Thorsen and F. C. Krebs, *Sol. Energy Mater. Sol. Cells*, 2010, **94**, 1553–1571.
33 A. Anctil, C. W. Babbitt, R. P. Raffaelle and B. J. Landi, *Environ. Sci. Technol.*, 2011, **45**, 2353–2359.
34 K. Petritsch, J. J. Dittmer, E. A. Marseglia, R. H. Friend, A. Lux, G. G. Rozenberg, S. C. Moratti and A. B. Holmes, *Sol. Energy Mater. Sol. Cells*, 2000, **61**, 63–72.
35 L. Schmidt-Mende, A. Fechtenkötter, K. Müllen, E. Moons, R. H. Friend and J. D. MacKenzie, *Science*, 2001, **293**, 1119–1122.
36 A. Sharenko, C. M. Proctor, T. S. van der Poll, Z. B. Henson, T.-Q. Nguyen and G. C. Bazan, *Adv. Mater.*, 2013, **25**, 4403–4406.
37 G. D. Sharma, P. Balraju, J. A. Mikroyannidis and M. M. Stylianakis, *Sol. Energy Mater. Sol. Cells*, 2009, **93**, 2025–2028.
38 B. Walker, X. Han, C. Kim, A. Sellinger and T.-Q. Nguyen, *ACS Appl. Mater. Interfaces*, 2012, **4**, 244–250.
39 S. Ma, Y. Fu, D. Ni, J. Mao, Z. Xie and G. Tu, *Chem. Commun.*, 2012, **48**, 11847–11849.
40 Y. He, H.-Y. Chen, J. Hou and Y. Li, *J. Am. Chem. Soc.*, 2010, **132**, 1377–1382.
41 C. J. Brabec, A. Cravino, D. Meissner, N. S. Sariciftci, T. Fromherz, M. T. Rispens, L. Sanchez and J. C. Hummelen, *Adv. Funct. Mater.*, 2001, **11**, 374–380.
42 A. M. Goodman and A. Rose, *J. Appl. Phys.*, 1971, **42**, 2823–2830.
43 Y. Li, *Acc. Chem. Res.*, 2012, **45**, 723–733.

